Chalcogenide Letters Vol. 19, No. 6, June 2022, p. 439 - 445

Chalcogenide glassy semiconductors of the system As-Se-S-Sn for X-ray imaging

A. Chirita*, V. Prilepov
Semiconductors Physics and Devices Laboratory, Physics and Engineering Faculty, Moldova State University, Chisinau, Republic of Moldova

The polymer/As-Se-S-Sn structure for X-ray imaging has been investigated. The possibility of registering relief-phase images for X-ray radiation of 0,154 nm was shown.

(Received March 23, 2022; Accepted June 20, 2022)

Keywords: x-ray imaging, chalcogenide glassy semiconductors, thermoplastic

1. Introduction

Chalcogenide glassy semiconductors (CGS) of the system As-Se-S are very promising materials for use in the registration of optical information. A wide range of carriers and methods for recording optical information was developed and studied based on these materials. Chalcogenide glassy semiconductors are sensitive materials to electron-beam recording [1-3], photoinducted transformation (photodarkening, photorefraction) [4-6], and as photoresist materials sensitive in UV-visible regions [7]. The surface relief formation (mass-transport effect) in the glassy materials of the system As-Se-S under non-uniform illumination is presented in works [8-9]. The photo-thermoplastic carriers, based on As-Se-S-Sn, for real-time holography and interferometry [10] have high values of resolution power - up to 4000 mm^{-1} [11], diffraction efficiency - up to 40% [12], and the real-time of the image formation 1–3 s [13]. The As_2S_3 thin films, as photoresists for x-ray photolithography, were studied in work [14]. As was shown in this work, the maximum sensitivity of As_2S_3 to X-rays is in the spectral range λ=2-7 nm. In [15], As_2S_3 thin films were studied as photoresist in shorter X-rays wavelength λ=0,1-0,6 nm, where their sensitivity is lower and large exposures are required. This work aimed to expand the area of application of chalcogenide glassy semiconductors for x-ray imaging.

2. Experimental setup

The carriers for x-ray imaging were obtained on a flexible polyethylene terephthalate film (PET) substrate (1, Fig.1a) which was covered with a semitransparent chrome electrode (2). The sensitive layer (3) based on chalcogenide glassy semiconductors 65at%$(As_2S_3)_{0,985}(SnSe)_{0,015}$:35at.% As_2Se_3 with a thickness of 1,6 μm was deposited onto the metal electrode by vacuum thermal deposition [16]. The composition of the semiconductor layer was selected experimentally, based on bibliographic data, where the properties of CGS based on As-Se-S doped with a small percentage of Sn were studied [17-18]. In the work [19] was shown that for the composition $(As_2S_3)_{0,3}(As_2Se_3)_{0,7}$,doped with Sn in the range of 0,015–0,030 at.%, the maximum of photoconductivity is observed at 0.02 at.% of tin. Photothermoplastic carriers based on the As-Se-S system doped with Sn have a high sensitivity (10^6 cm^2/J) for relief-phase holograms recording [20] and 10^4 cm^2/J for impulse holograms recording in the nanosecond range [21]. The thermoplastic layer of butilmetacrylate-styrene (4) with a thickness of 0,6 μm was deposited on the semiconductor layer.

* Corresponding author: arc_chirita@yahoo.com
https://doi.org/10.15251/CL.2022.196.439

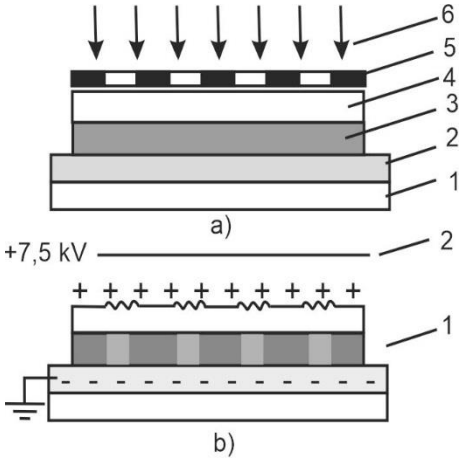

Fig.1 a) 1.Polyethylene terephthalate film, 2. Chrome electrode, 3.Semiconductor layer, 4. Thermoplastic polymer, 5. Brass mesh, 6. X-ray beam; b) 1.Irradiated carrier, 2. High voltage corona charging

The installation based on an x-ray tube with a copper anode (voltage 45 kV, current 40 mA) was used for experiments. The samples were irradiated with a parallel x-ray beam 20x1,5 mm and close to the monochromatic wavelength of λ~0,154 nm ($K_{\alpha 1,\alpha 2}$ ~8.04keV). For registration in the visible region of the spectrum the monochromatic laser radiation λ=532 nm was used. A brass mesh was used as a mask for x-ray image recording using the contact method. The mask was placed onto the surface of the thermoplastic layer (5, Fig.1a) and irradiated with visible or x-ray irradiation (6) for a fixed time. Unlike the photothermoplastic process, when illumination and registration are carried out simultaneously [22], in this experiment the carrier is removed from the x-ray chamber after irradiation for the next step of image visualization, as was proposed in work [23]. As was shown in this work, the resistivity of the semiconductor layer is modulated in the irradiated areas. The carrier is heated up to a vicious state of the thermoplastic layer ($T=68^0C$) in darkness. The heated-up carrier is charged for 2,5-3,6 s with a high voltage (7,5 kV) corona charging (2, Fig.1b). The surface of the thermoplastic is charged with positive air ions, and the conductivity of the semiconductor layer in the irradiated areas is higher due to the change of resistivity under irradiation [23]. Positive charges on the surface and negative charges in the semiconductor layer deform the thermoplastic under the Coulomb interaction [10]. Thus, a relief-phase image of the registered object is formed [13].

3. Results

Fig.2a shows the zoomed image of the brass mesh that was used as a mask (5, Fig.1) for the registration of x-ray images. After the thermoplastic visualization, the recorded images were studied on an optical microscope in reflected light.

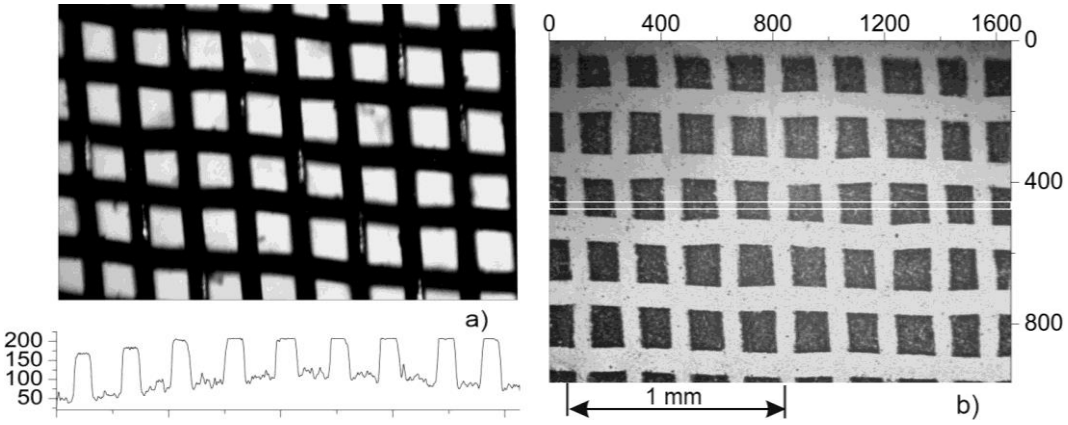

Fig. 2. a) The brass mesh, used as a mask, b) x-ray image recorded at exposure of 5,1 J/cm^2.

Fig.2b shows an image of a brass mesh obtained at an X-ray exposure of 5,1 J/cm^2. As can be seen from Fig. 2b, the thermoplastic process forms a negative image of the original object. Thermoplastic visualization (Fig.1b) was carried out at temperature T=68^{0}C, voltage 7,5 kV, and charging time t=2,5 s. At an optical magnification of 1200^X, the edge of one of the squares of the mesh (Fig.3) shows deformation of the thermoplastic surface in the irradiated areas.

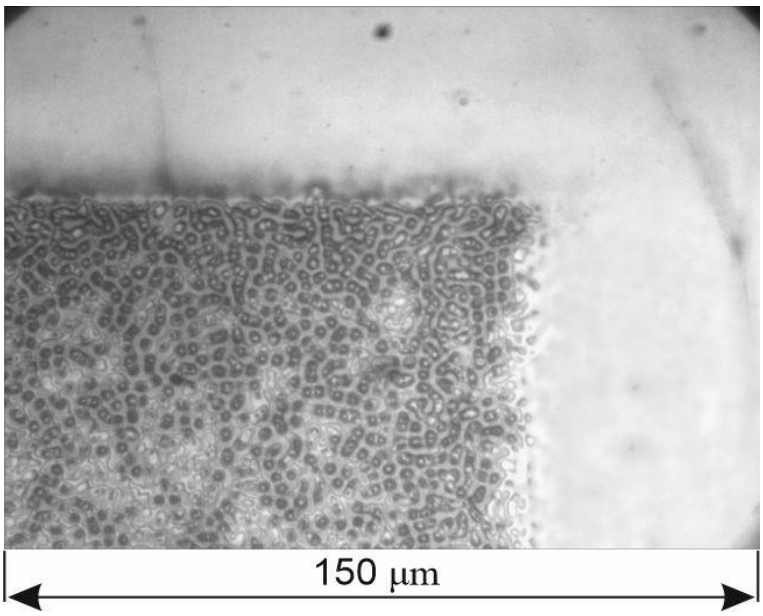

Fig. 3. Zoomed image of the irradiated and non-irradiated areas.

The image in Fig.2b was processed by a graphical editor to allow defining the pixel-by-pixel distribution of the grayscale brightness along with the frame. Through the image center, a 20-px-thick band (white lines, Fig. 2b) was picked out by scanning along the frame. Figure 2b shows the pixels brightness distribution (from 0 to 255 of the grayscale) in light and dark places of the recorded image. The Michelson formula is used to determine the image contrast:

$$k = \frac{I_{max} - I_{min}}{I_{max} + I_{min}} \quad (1)$$

where I_{max} and I_{min} are the brightness of the dark and light areas of the image obtained from the pixels brightness distribution (Fig.2b). For an image recorded at an exposure of 5,1 J/cm^2, the

average image contrast was k=0,24. When the exposure decreases to 3,36 J/cm^2 the time of high voltage corona charging increases to t=2,8 s.

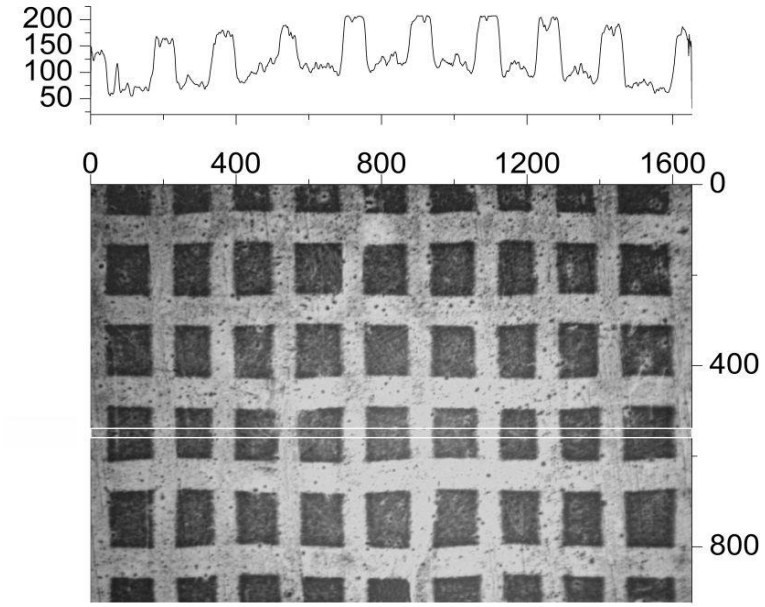

Fig.4 X-ray image recorded at exposure of 3,36 J/cm^2

The increase of noise is observed both in the irradiated and non-irradiated areas of the image (Fig.4). The average image contrast is k=0,16. To register images at an exposure of 2,52 J/cm^2 (Fig.5), the high-voltage charging time increased to t=3,6 s. The image shows an increase of noise in both irradiated and non-irradiated areas of the image.

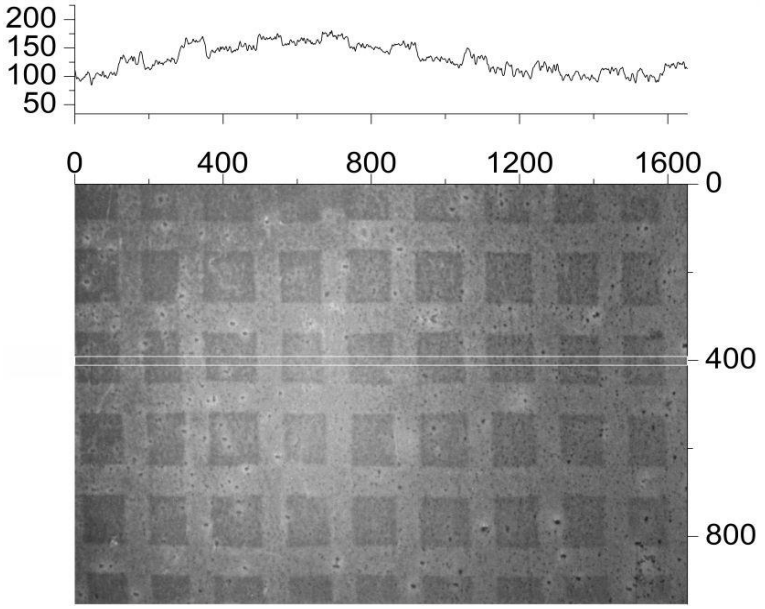

Fig.5 X-ray image recorded at exposure of 2,52 J/cm^2.

It is still possible to distinguish the outlines of the original object on the registered image, but the average contrast of the image is no more than k=0,02.

Fig.6 shows the contrast of the registered images depending on the X-ray exposure.

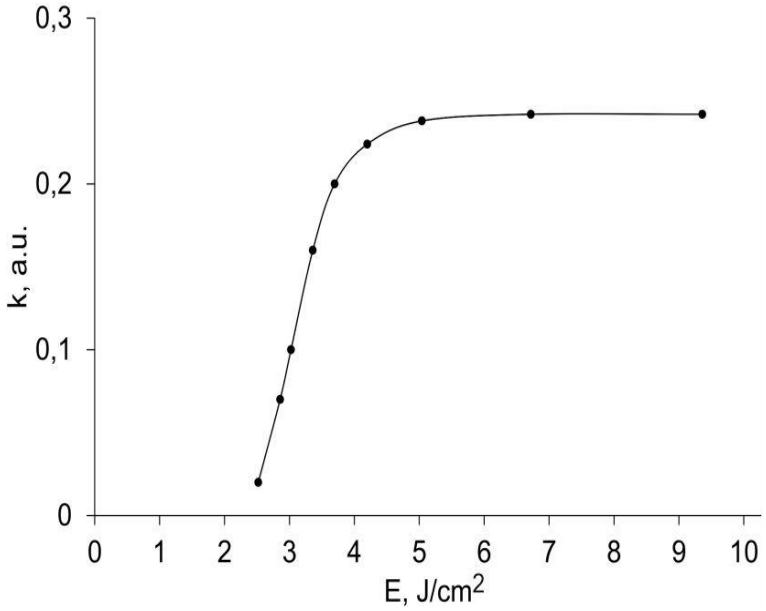

Fig. 6. Contrast versus exposure.

As can be seen from Fig.6, the maximum image contrast k=0,24 is achieved at an exposure close to 5,1 J/cm^2. The maximum contrast k=0,24 is a typical value for relief-phase images in photothermoplastic recording [14].

For comparison with X-rays, carriers were investigated for visible light imaging. Similar to the previous experiments, the carriers were illuminated through a mask with monochromatic radiation λ=532 nm at an intensity of 45 mW/cm^2. Thermoplastic visualization was carried out under the same conditions as for X-rays imaging. Images with contrast of k=0,24 were obtained at an exposure of 270 mJ/cm^2 (exposure time t=6 s). To study these carriers in a photothermoplastic recording, an image of a brass meshd was projected onto the carrier using an optical system. Images were recorded with contrast k=0,24 in laser radiation λ=532 nm at an exposure of 10^{-6} J/cm^2, which is a typical value for photothermoplastic recording process [20-22].

The effect of photostructural changes (photodarkening, photorefraction) in chalcogenide glassy semiconductors under the action of optical radiation is well known from the literature [8, 25–26]. This effect was not detected during X-ray irradiation of the investigated carriers. For research, a semiconductor layer was deposited on a sapphire substrate to exclude the effect of X-rays on the PET substrate. Measurement of the spectral dependence of transmission before and after X-ray irradiation at exposures up to 5,1 J/cm^2 showed no change in the optical transmittance of the samples under study.

It was not possible at this stage to study the obtained carriers for recording X-ray images by photothermoplastic recording when the image is recorded directly during irradiation. The X-ray installation does not allow the use of high voltage (7,5 kV) corona charging inside the X-ray chamber. These studies are the goal of future experiments.

4. Discussions

The studies showed the sensitivity of the chalcogenide glassy semiconductors of the 65at%$(As_2S_3)_{0,985}(SnSe)_{0,015}$:35at.% As_2Se_3 system for imaging in visible light and X-ray radiation at the wavelength of λ=0,154 nm. Thermoplastic development showed the presence of structural changes in the X-ray irradiated areas of the CGS, which modulates the resistivity of the semiconductor layer. The deformation of the thermoplastic layer in the irradiated areas takes place both under illumination of λ=532 nm and under X-ray irradiation. Photoinduced changes in CGS (photodarkening, photobleaching) under the optical radiation are well studied [7, 25–26].

However, no change in the optical transmittance in the CGS layer under X-rays irradiation (at exposures up to 5,1 J/cm^2) was detected. According to the literature data, a change in the optical properties of CGS was found under the γ-radiation, which is presented in [27–28]. However, the darkening in the layers based on As-S was observed upon irradiation with hard γ-quanta (1,25 MeV) and at high radiation doses - up to 10 MGy. At this stage of research, it can be assumed that when the studied CGS layers are irradiated with X-ray radiation λ = 0,154 nm at exposures up to 5,1 J/cm^2, structural changes occur that change the resistivity in the layer, but no changes in optical transmission were observed. The exposure interval for X-ray recording on the investigated media is 2,52-5,1 J/cm^2, which shows a higher sensitivity compared to X-ray lithography for the range λ=0,1-0,6 nm. As was shown in work [15], the As_2S_3 in this wavelength range requires exposures of 25–50 J/cm^2. The effect of structural changes in CGS under the X-ray radiation of λ=0,154 nm requires a more detailed study, what was not the purpose of this work. At this stage, only experimental results to use CGS in the registration of X-ray images were obtained.

5. Conclusions

The carriers based on the polymer/As-Se-S-Sn structure make it possible to record images both in the visible spectral range and using the X-ray at a wavelength of 0,154 nm. Thermoplastic visualization forms a relief-phase image of the registered object with low contrast values of k=0,02-0,24. However, relief-phase carriers are successfully used to record holographic images with high diffraction efficiency [12, 20] and resolution power [23]. X-ray holography may be the most promising way to use the proposed carriers.

Acknowledgements

This research was funded by the National Agency for Research and Development of the Republic of Moldova, grant 20.80009.5007.12

References

[1] M. Iovu, S. Sergeev, O. Iaseniuc, Optoelectron. Adv. Mat. **12**(7-8), 377 (2018).

[2] O. Iaseniuc, M. Enachescu, D. Dinescu, M. Iovu, S. Sergheev, J. Optoelectron. Adv. M. **18**(1-2), 34 (2016).

[3] S. Sergeev, M. Iovu, A. Meshalkin, Chalcogenide Letters 17(1), 25 (2020)

[4] O. Iaseniuc, I. Cojocaru, A. Prisacar, A. Nastas, M. Iovu, Journal of Optics and Spectroscopy 121(1), 1128 (2016); https://doi.org/10.1134/S0030400X16070237

[5] A. Nastas, A. Andriesh, V. Bivol, A. Prisakar, G. Tridukh, Technical Physics Letters 32(1), 45 (2006); https://doi.org/10.1134/S1063785006010159

[6] A. Nastas, A. Andriesh, V. Bivol, A. Prisakar, G. Tridukh, Technical Physics 54(2), 305 (2009); https://doi.org/10.1134/S1063784209020236

[7] J. Teteris, M. Reinfelde, Journal of Optoelectronics and Advanced Materials 5(5), 1355 (2003)

[8] E. Achimova, A. Stronski , V. Abaskin, A. Meshalkin, A. Paiuk, A. Prisacar, P. Oleksenko, G. Triduh, Optical Materials 47, 566 (2015); https://doi.org/10.1016/j.optmat.2015.06.044

[9] V. Cazac, A. Meshalkin, E. Achimova, V. Abashkin, V. Katkovnik, I. Shevkunov, D. Claus, and G. Pedrini, Applied Optics 57, 507 (2018); https://doi.org/10.1364/AO.57.000507

[10] A. Chirita, N. Kukhtarev, T. Kukhtareva, O. Korshak, V. Prilepov, Journal of Modern Optics 59(16), 1428 (2012); https://doi.org/10.1080/09500340.2012.719936

[11] A. Chirita, N. Kukhtarev, T. Kukhtareva, O. Korshak, V. Prilepov, Laser Physics 23, 036002 (2013); https://doi.org/10.1088/1054-660X/23/3/036002

[12] I. Andries, T.Galstian, A.Chirita, J. Optoelectron. Adv. M. **18**(1-2), 56 (2016).

[13] A. Chirita, V. Prilepov, M. Popescu, I. Andries, M. Caraman, Iu. Jidcov, J. Optoelectron. Adv. M. **17**(7-8), 925 (2015).

[14] G. Danev, E. Spassova, J. Assa, P. Guttmann, Advanced materials for optics and electronics 8, 129 (1998); https://doi.org/10.1002/(SICI)1099-0712(199805/06)8:3<129::AID-AMO331>3.0.CO;2-5

[15] A. Buroff, A. Rush, Journal of Non Crystalline Solids 90, 585 (1987); https://doi.org/10.1016/S0022-3093(87)80491-X

[16] V. Prilepov, M. Popescu, A. Chirita, O. Korshak, P. Ketrush, N. Nasedchina, Chalcogenide Letters 10(7), 249 (2013)

[17] M. Popescu, Chalcogenide Letters 1(12), 145 (2004)

[18] P. Boolchand, D. Georgiev, M. Iovu, Chalcogenide Letters 2(4), 27 (2005)

[19] I. Burdiyan, I. Feshchenco, Inorganic Materials 41(9), 1013 (2005) https://doi.org/10.1007/s10789-005-0254-2

[20] A. Chirita, T. Galstian, M. Caraman, V. Prilepov, O. Korshak, I. Andries, Optoelectron. Adv. Mat. **7**(3-4), 293 (2013).

[21] A. Chirita, F. Dimov, S. Pradhan, P. Bumacod, O. Korshak, Journal of Nanoelectronics and Optoelectronics 7(4), 415 (2012); https://doi.org/10.1166/jno.2012.1321

[22] A. Chirita, V. Prilepov, M. Popescu, O. Corsac, P. Chetrus, N. Nasedchina. Optoelectron. Adv. Mat. **9**(7-8), 919 (2015).

[23] A.Nastas, A. Andriesh, V. Bivol, I. Slepnev, A. Prisakar, Technical Physics Letters 35(4), 375 (2009); https://doi.org/10.1134/S1063785009040269

[24] Y. Cherkasov, Proc. SPIE 3347, 101 (1998)

[25] J. De Neufville, S. Moss, S. Ovshinsky, Journal of Non-Crystalline Solids 13, 191(1973); https://doi.org/10.1016/0022-3093(74)90091-X

[26] T. Uchino, D. Clary, Physical Review Letters 85(15), 3305 (2000); https://doi.org/10.1103/PhysRevLett.85.3305

[27] O. Shpotyuk, A. Matkovskii, Journal of Non-Crystalline Solids 176, 45 (1994); https://doi.org/10.1016/0022-3093(94)90209-7

[28] M. Shpotyuk, A. Kovalskiy, R. Golovchak, O. Shpotyuk, Journal of Non-Crystalline Solids 498, 315 (2018); https://doi.org/10.1016/j.jnoncrysol.2018.04.006